$\Sigma\Delta$ Effects and Charge Locking in Capacitive MEMS under Dielectric Charge Control

Panagiotis Giounanlis[1*], Sergi Gorreta[2], Manuel Dominguez-Pumar[2], Joan Pons-Nin[2], Orla Feely[1], Elena Blokhina[1]

[1] School of Electrical and Electronic Engineering, University College Dublin, Ireland
[2] Micro and Nano Technologies Group, Universitat Politecnica de Catalunya, Spain

[1*] corresponding author email: panagiotis.giounanlis@ucdconnect.ie

***Abstract*—This work investigates, analytically and experimentally, the effects induced by the use of a first-order sigma-delta feedback loop as a control method of dielectric charging for capacitive MEMS. This technique allows one to set a desired level of net charge in the dielectric of a MEMS device by continuously alternating the polarity of the actuation voltage. This control system displays a number of interesting effects, inherited from sigma-delta modulation, and not usually found in conventional MEMS applications, with the charge locking phenomenon being the most relevant. The convergence time and the effectiveness of the control method are also investigated and discussed.**

I. Introduction

Dielectric charging is a major reliability issue in electrostatic microelectromechanical systems (MEMS) [1], [2]. For instance, this problem hinders the large scale use of these devices as variable capacitors, switches or oscillators in applications such as components for RF. In the case of varactors and voltage-actuated switches, thin dielectric layers are commonly used to prevent short-circuiting between moveable and fixed parts. However, the application of relatively high voltages across such small scale structures results in high electric fields, which may produce such phenomena as dielectric polarization or charge injection and trapping. Such dielectric charging caused by device actuation produces undesired changes in key parameters of the device, such as: pull-in voltage drift, capacitance–voltage $C(V)$ characteristic shifts or, in severe cases, permanent stiction of mechanical parts.

In recent years, smart actuation techniques and strategies to mitigate or control the effects of dielectric charging in MEMS capacitors have been proposed [3]–[8]. Closed-loop strategies are inspired by sigma-delta ($\Sigma\Delta$) modulation: they trace a certain characteristic of the MEMS that is related to the dielectric charge and dynamically apply correcting feedback stimuli. Studies [7], [8] experimentally implement first and second-order $\Sigma\Delta$ modulation on MEMS, while [9] realises an ASIC first-order $\Sigma\Delta$ control. These studies focus on experimental validation or on IC implementation of control. However, an analytical or extended numerical analysis of these systems is an open issue. They are impeded by the lack of simple but reliable models of dielectric charging and mechanical structures. In addition, one has to analyse the entire system "capacitive MEMS – dielectric – feedback loop", which is a non-trivial task. As a matter of fact, no rigorous proof of the robustness of the $\Sigma\Delta$ loop for MEMS has been presented so far. Discussions on undesirable effects that may appear in the dynamics of MEMS due to the feedback loop are very limited.

This work addresses the robustness of the first-order $\Sigma\Delta$ loop and its effects (the convergence time, charge locking and general stability) on MEMS. From our analysis, we predict how the $\Sigma\Delta$ effects can be measured and provide experimental validation. The experimental validation is a rather remarkable result since these effects appear in a realistic physical system that involves components belonging to different physical domains. The appearance of channel tones, which is another well-known $\Sigma\Delta$ related phenomenon is not investigated in this work. These tones may be considered a secondary issue since they only affect the capability of the method to retrieve the information on dielectric charging, but not the capability of the method to fix a desirable level of charge.

II. Statement of the problem

The aim of this study is not to introduce a new charge control and actuation technique for MEMS. Rather we investigate it, providing an analysis of its dynamics, as stated in the Introduction, and validating our results experimentally. Therefore, we focus on the first-order $\Sigma\Delta$ control of dielectric charge from [7], [10].

Let us first provide a brief overview of the system, shown in Fig. 1. A MEMS capacitor is the one used in the experimental part of this work. It is a movable plate-electrode suspended in air above a fixed plate-electrode that has a dielectric layer deposited on top. More details about this device are given in Sec. V. The net charge stored in the dielectric, Q_d, changes the effective voltage "seen" by the device by the amount $V_{\text{shift}} = Q_d/C_d$, where C_d is the capacitance of the dielectric layer. This implies that Q_d causes a horizontal shift of the capacitance-voltage characteristic $C(V)$ of the device. In the control system, V_{shift} (then, Q_d) is calculated from a quasi-differential capacitance ΔC measurement, obtained at sampling times nT_s. On the other hand, one of the two bipolar voltage waveforms BIT0 and BIT1, described in Fig. 1, is applied to the device during each sampling period. The application of either BIT0 or BIT1 produces opposite (but not necessarily symmetrical) $C(V)$ shifts. Thus, causing opposite effects on the charge dynamics. The control method compares ΔC with a preselected threshold ΔC_{th} (thus with a threshold Q_{th}) and decides which waveform must be applied in the next sampling period to achieve $Q_d = Q_{\text{th}}$.

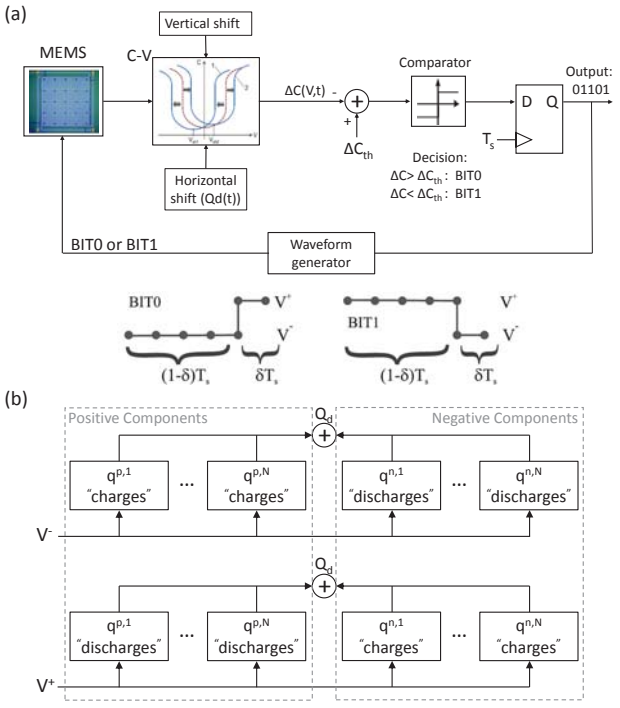

Fig. 1: (a) Block diagram of the system and the description of the voltage waveforms, BIT0 and BIT1, used to actuate the MEMS. The electrostatic actuation alters the net charge trapped in the MEMS dielectric, causing a horizontal shift of the $C(V)$ characteristic of the device. Other factors, such as the distribution of charge, contribute to vertical shift of the $C(V)$. (b) Effect of actuation voltages on the dielectric charge. The charging process consists of multiple positive and negative components defined by eq. (1). They can be seen as "capacitors" with different charge and discharge dynamics. When one applies BIT0, the positive components charge more than the negative ones (depending on the δ value). For the BIT1 waveform the effect is opposite. The total charge is obtained by summing all components up.

A. Electromechanical model

The MEMS is actuated by applying a voltage V across its electrodes. This causes a displacement y of the moveable electrode and, as a consequence, a change in the device capacitance $C(y)$. In a 1D approach, the kinetics of the moveable electrode can be described by a typical mass-spring-damping differential equation $m\ddot{y}(t)+b\dot{y}(t)+ky(t)=F_{\text{el}}(V,y)$, where m is the mass of the movable electrode, b is the damping factor, k is the spring coefficient of the mechanical restoring force and $F_{\text{el}}(V,y)$ is the electrostatic force. However, the electromechanical part of the system can be described with the desired complexity, depending on the accuracy required, i.e. using partial differential equations or finite-element methods. Therefore, the total capacitance C of the device will be a function of the form $\mathcal{F}=\mathcal{C}(\mathcal{Y})$, where $\mathcal{Y}$ expresses the position of the moveable electrode.

All the simulations in this work have been performed using both 1D models and beam models (partial differential equations), taking into account the presence of both uniform and various non-uniform charge distributions [11]. The latter modifies the electrostatic force F_{el} that acts on the MEMS, making it proportional to $(V-V_{\text{shift}})^2+\sigma_V^2$ where σ_V^2 is the variance of the dielectric charge distribution. Thus, if the charge is accumulated in the dielectric uniformly, there is no vertical shift of $C(V)$.

B. Charge dynamics model

Let us consider the multi-exponential model for the dielectric charge dynamics experimentally validated in [12], [13]. This model considers a set of positive $q^p=\sum_i q^{p,i}$ and negative $q^n=\sum_i q^{n,i}$ charge components:

$$q^p(t)=\begin{cases}Q^p_{max}\sum_i \zeta_i^p e^{-t/\tau^p_{Di}} & V>0\\ Q^p_{max}(1-\sum_i \zeta_i^p e^{-t/\tau^p_{Ci}}) & V<0\end{cases}$$
$$q^n(t)=\begin{cases}Q^n_{max}(1-\sum_i \zeta_i^n e^{-t/\tau^n_{Ci}}) & V>0\\ Q^n_{max}\sum_i \zeta_i^n e^{-t/\tau^n_{Di}} & V<0\end{cases} \quad (1)$$

where Q^p_{max} and Q^n_{max} are respectively the maximum value of the positive and of the negative charge components for the voltage applied V, τ_{Ci} and τ_{Di} are charging and discharging time constants and ζ_i are coefficients expressing the contribution of each exponential to each charge component (then, $\sum_i \zeta_i = 1$ for each component). The time varying expression of the total dielectric charge is $Q_d(t)=q^p(t)+q^n(t)=\sum_i q^{p,i}(t)+\sum_i q^{n,i}(t)$, which is the sum of multiple *independent* charge components.

C. Closed-loop control algorithm of dielectric charging

The control method is based on measurements of the quasi-differential capacitance ΔC, which under some conditions can be easily related to the net dielectric charge Q_d. For instance, for a device working below pull-in, with a parabolic bottom of the $C(V)$ and symmetrical voltages in BIT0 and BIT1 waveforms ($V^+=-V^-=V$, see Fig. 1), it is

$$\Delta C(t)=-4\alpha V Q_d(t)/C_d \quad (2)$$

where the coefficient α is obtained from fittings of the $C(V)$. From the current value of ΔC, the control method is aimed at fixing the dielectric charge at a selected (desired) level Q_{th} by using this decision mechanism:

$$\text{BIT}((n+1)T_s)=\begin{cases}\text{BIT0} & \Delta C(nT_s)>\Delta C_{\text{th}}\ \ (Q_d(nT_s)<Q_{\text{th}})\\ \text{BIT1} & \Delta C(nT_s)<\Delta C_{\text{th}}\ \ (Q_d(nT_s)>Q_{\text{th}})\end{cases} \quad (3)$$

where T_s is the sampling time, $Q_d(nT_s)$ is the total dielectric charge estimated from the quasi-differential capacitance $\Delta C(nT_s)$ measured at $t=nT_s$, and $\text{BIT}((n+1)T_s)$ is the voltage waveform, BIT0 or BIT1, to apply to the MEMS in the next sampling period $[nT_s,(n+1)T_s)$.

The dynamics of the total charge can be expressed in a compact form, where for simplicity we consider $f(nT_s)=f_n$, as follows:

$$Q_{n+1}=\Theta(Q_n,b_n),\quad b_{n+1}=\tfrac{1}{2}(1+\text{sgn}(\Delta C_{\text{th}}-\Delta C_n)) \quad (4)$$

where $Q_{n+1}\,\epsilon\,\mathcal{R}$ is the net charge in the next sampling period as a function of its current value Q_n and of the decision bit provided by (3): $b_n\,\epsilon\,\mathcal{B}=\{1,0\}$. Thus, we will use the subscript n to denote the discrete-time evolution of the dynamical

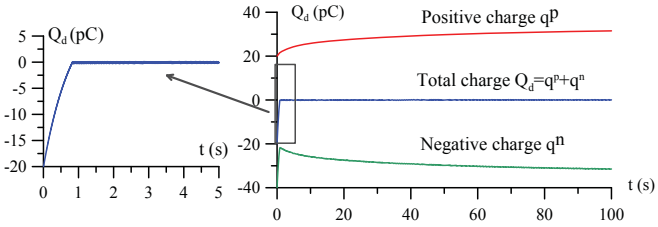

Fig. 2: Simulation results showing the evolution of the positive and negative charge components and of the total charge when the control method with Q_{th}=0 is applied. The initial net charge is negative.

quantities in our problem. The script i will be used to denote a quantity related to individual charge components. Note that the dependence of the system dynamics on the equation of the mechanical component is hidden in b_n. Equations (4) represent a piecewise contraction map that is asymptotically periodic, i.e. its steady state solutions are stable cycles [14].

III. Global behaviour of the ΣΔ controlled MEMS

A. Convergence time of the multiple-charge components

The charge dynamics are modelled as a sum of independent components, each evolving with its own time constants. If we look separately at the positive and negative components of Q_d, they evolve and reach a steady state rather slowly, as shown in the simulation results of Fig. 2. This is determined by the largest characteristic time scale of q^p and q^n, which can be in the range of hours or even days. However, the total charge $Q_d = q^n + q^p$ evolves with noticeably faster time scales. This is a very useful property, since it allows one to fix the desired level of dielectric charge faster. In the experiment described in Sec. V, the total charge settles to the desired level faster than the characteristic time of individual charge components.

B. Devil's staircase and charge locking

Similarly to ΣΔ modulators, the amount of charge in the dielectric can be inferred from the averaged output bitstream $\overline{b}$, that tells us what is the average decision bit applied by the control loop. After the system has reached a steady state, the averaged bitstream corresponds to a stable cycle of dielectric charge. When the desired level of charge is changed (by adjusting ΔC_{th}), a change in the averaged bitstream should be observed. Ideally, the plot $\overline{b}(\Delta C_{th})$ should be a straight line. As shown in Fig. 3(a), this is the case when a small sampling time T_s is used. However, when T_s becomes comparable with the fastest time constant of the charge dynamics, plateaus appear in the plot $\overline{b}(\Delta C_{th})$.

Such a plot is a *Devil's staircase*, an effect previously seen and explained in the context of conventional ΣΔ modulators [15], where plateaus are associated with integrator leakage. In our case, T_s can be associated with the leakage of the dielectric charge reservoir, understood as an integrator in the ΣΔ loop [7]. This generates the appearance of increasing plateaus with increasing T_s. Clearly, this is an undesirable effect that should be avoided by proper selection of the sampling time T_s. The case of non-uniform distributions of charge was also investigated. The results, reported in Fig. 3(a), demonstrate that the Devil's staircase effect also persists in this case.

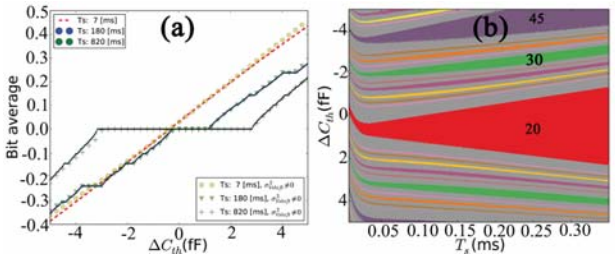

Fig. 3: (a) Simulation results of the averaged bitstream ($\overline{b}$) provided by the control loop as a function of ΔC_{th} for both uniform and non-uniform charge distributions. Each point corresponds to a steady-state case. (b) Domains of existence of cycles observed in the system.

The Devil's staircase is a manifestation of a more general phenomenon termed here as *charge locking*. By varying two parameters, for instance, T_s and ΔC_{th}, the results of Fig. 3(b) are obtained. This graph shows the average amount of charge fixed by the control algorithm in the MEMS dielectric. Each colored tongue corresponds to a case where this charge is fixed, or *locked*, to the same value.

These plateaus disappear if a second-order feedback loop is employed [8]. However, the implementation of the second-order loop for MEMS may be difficult. One should consider all trade-offs between a simpler but less reliable first-order ΣΔ loop and a higher-complexity and more reliable second-order loop.

IV. Analytical properties of the control method

Followed on from our discussion of some typical effects of ΣΔ loops, let us now focus on the global convergence and the robustness of the charge control algorithm.

A. Analysis of the discrete time model

The charge difference ΔQ_0, extracted or added to the dielectric by the feedback loop after applying BIT0 is:

$$\begin{aligned}\Delta Q_0 = Q_d(n+1) - Q_d(n) = \sum_i q_n^{p,i}\alpha_{C,i}^{1-\delta}\alpha_{D,i}^{\delta} + \\ + \sum_i \zeta_i^{p,i} Q_{max}^{p}(1-\alpha_{C,i}^{1-\delta})\alpha_{D,i}^{\delta} + \sum_i q_n^{n,i}\beta_{D,i}^{1-\delta}\beta_{C,i}^{\delta} \\ + \sum_i \zeta_i^{n} Q_{max}^{n}(1-\beta_{C,i}^{\delta}) - q_n^p - q_n^n\end{aligned} \quad (5)$$

where $\alpha_{C,D,i} = \exp[-\frac{T_s}{\tau^p_{C,D,i}}]$ and $\beta_{C,D,i} = \exp[-\frac{T_s}{\tau^n_{C,D,i}}]$. ΔQ_0 can be seen as sum of positive and negative charge differences due to the application of a BIT0: $\Delta Q_0 = \Delta Q_0^p + \Delta Q_0^n$. A similar expression for ΔQ_1 can be found when a BIT1 is applied.

Now, let us consider that T_s is far below the fastest time constant of the charge dynamics. This assumption allows us to linearise and discretise expressions (1). According to this, let us examine separately the positive and negative components of (5) for the case of BIT0:

$$\Delta Q_0^{p,i} = Q_{max}^{p,i}\frac{(1-\delta)T_s}{\tau_{Ci}^p}\left[1 - \frac{q^{p,i}}{Q_{max}^{p,i}}\left(1 + \frac{\delta\tau_{Ci}^p}{(1-\delta)\tau_{Di}^p}\right)\right] \quad (6)$$

$$\Delta Q_0^{n,i} = Q_{max}^{n,i} \frac{\delta T_s}{\tau_{Ci}^n} \left[1 - \frac{q^{n,i}}{Q_{max}^{n,i}} \left(1 + \frac{(1-\delta)\tau_{Ci}^n}{\delta \tau_{Di}^n}\right)\right] \quad (7)$$

where $Q_{max}^{p,i} = Q_{max}^p \zeta_i^p$ and $Q_{max}^{n,i} = Q_{max}^n \zeta_i^n$.

Similar expressions can be easily derived for BIT1 ($\Delta Q_1^{p,i}$ and $\Delta Q_1^{n,i}$). Then, the system evolution can be described with the following 2D map $G : R^2 \to R^2$:

$$\begin{aligned} q_{n+1}^{p,i} &= q_n^{p,i} + \Delta Q_0^{p,i}(1-b_n) + \Delta Q_1^{p,i} b_n \\ q_{n+1}^{n,i} &= q_n^{n,i} + \Delta Q_0^{n,i}(1-b_n) + \Delta Q_1^{n,i} b_n \end{aligned} \quad (8)$$

where $q_n^p, q_n^n \in \mathbb{R}$, $n \in \mathbb{N}$ and the applied bit $b_n \in \mathcal{B} = \{0, 1\}$.

Taking into account that both voltage polarities (V^+ and V^-) are applied during a certain time in BIT0 and BIT1, depending on the value of δ, the average time in which the positive voltage (V^+) is applied can be described as $\overline{b_{eff}} = \overline{b}(1-\delta) + (1-\overline{b})\delta$. And therefore, the average time for the negative voltage (V^-) is $1 - \overline{b_{eff}}$.

Now, it is possible to find the stable equilibrium point of each charge contribution of the system (8) as a function of δ and $\overline{b}$:

$$\begin{aligned} q^{p,i} &= Q_{max}^{p,i} \frac{(1-\overline{b_{eff}})}{\tau_{Ci}^p/\tau_{Di}^p \overline{b_{eff}} + (1-\overline{b_{eff}})} \\ q^{n,i} &= Q_{max}^{n,i} \frac{\overline{b_{eff}}}{\tau_{Ci}^n/\tau_{Di}^n (1-\overline{b_{eff}}) + \overline{b_{eff}}} \end{aligned} \quad (9)$$

Moreover, since the system is dissipative (contracting), all the trajectories are forced to converge to the stable equilibrium point (9).

Assuming now that the target charge surface has been reached, i.e. $Q_d = Q_{th}$, in the final equilibrium point we will have that:

$$Q_{th} = Q_d = \textstyle\sum_i q^{p,i} + q^{n,i} \quad (10)$$

and this equation implicitly determines the asymptotic value of the averaged $\overline{b}$.

Finally, the equation of a first order sigma-delta modulation can be obtained taking into account all the charge contributions presented in (8).

$$Q_d(n+1) = Q_d(n) + (1-b_n) \sum_i \Delta Q_0^i + b_n \sum_i \Delta Q_1^i \quad (11)$$

B. Effectiveness of the control method for a two-exponential charging model

Let us now use the analytical models derived in the previous section for the specific case of two exponentials in each charge component. The performance of the $\Sigma\Delta$ charge control algorithm is demonstrated in Fig. 4, where we plot ΔQ as a function of the initial charge state for each component, q_n^p and q_n^n. The diagonal line represents the condition where the total charge is as desired. In our example, this condition is $q_n^p + q_n^n = 0$, that is, the dielectric stays electrically neutral. Therefore, for all points lying on the upper-left half plane (UL) the total charge is positive and for those in the lower-right half plane (DR) the total charge is negative.

For the $\Sigma\Delta$ algorithm to converge, ΔQ must be positive in the lower half-plane and negative in the upper half-plane. In this case of ideal operation, the $\Sigma\Delta$ loop will compensate any

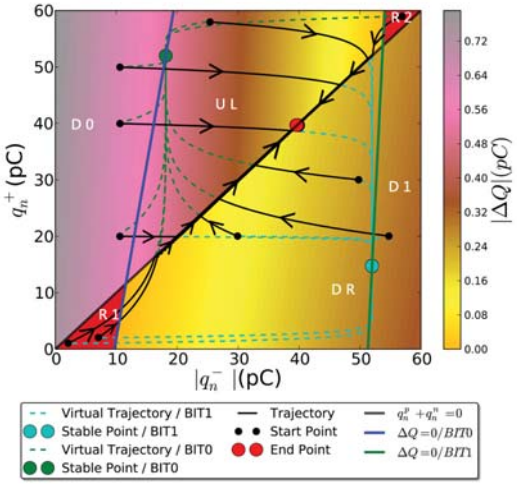

Fig. 4: Dynamics of the control algorithm in the (q_n^n, q_n^p) plane. If the total charge $Q_d = q_n^n + q_n^p$ is in the upper half-plane $D_0 \cup UL$, the control method changes the charge, moving it to the desired level set by the line $Q_d = Q_{th}$. If the total charge $Q_d = q_n^n + q_n^p$ is in the lower half-plane $D_1 \cup DR$, the control method again changes it towards the desired level. Once the line $Q_d = Q_{th}$ is reached, a sliding mode control takes place unless the point $\Delta Q_0 = |\Delta Q_1|$ is reached. The value of ΔQ is also shown in the plane for convenience.

excess of positive or negative charge in the dielectric. This is indeed so for the two largest portions of the plane, where the right conditions on ΔQ are fulfilled.

Figure 4 depicts the state of the system as a point moving along a trajectory in the plane. In the two largest sections of the plane, above and below the diagonal line that represents the desired level of charge, we proceed towards the diagonal line with every step of application of the algorithm. The system dynamics are dominated by the presence of the two stable points and the trajectories converge towards them, as desired.

However, in principle it is possible to observe the reverse behaviour of the $\Sigma\Delta$ algorithm. For example, the domains denoted as R1 and R2 in Fig. 4 correspond to the opposite behaviour where $\Delta Q < 0$ for BIT0 and $\Delta Q > 0$ for BIT1. In order to avoid the undesired behaviour of the algorithm, we must design the system accordingly, selecting small enough values of T_s and δ.

Finally, we note that as soon as a trajectory reaches the diagonal line, it undergoes a specific type of *sliding mode* control [16].

V. Experimental results

There are no means to directly measure the dielectric charge in a MEMS device while it is being used. Thus, it is extremely difficult to have an understanding of the dielectric charge dynamics without interfering into the operation of the device. However, our analysis predicts a number of $\Sigma\Delta$ effects when applying dielectric charge control. Then, if we can observe them experimentally, we can prove that our understanding of the charge behaviour is correct.

In this section, we demonstrate experimentally the charge locking phenomenon. To this effect, the $\Sigma\Delta$ charge control has

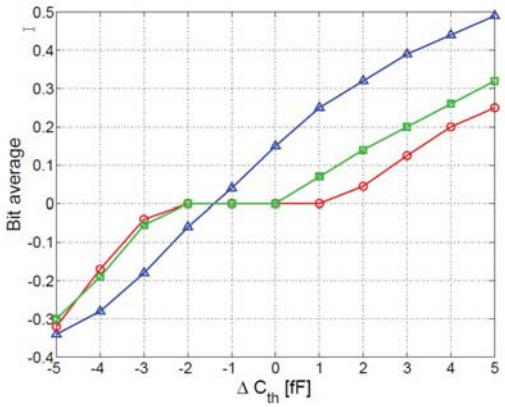

Fig. 5: Averaged bitstream versus target differential capacitance obtained experimentally for T_s=1.7 s (circles), 820 ms (squares) and 180 ms (triangles).

been applied to a MEMS capacitor that exhibits reasonably fast charging when working below pull-in. The device, fabricated with standard PolyMUMPS technology, is a two-parallel plate structure. The upper plate-electrode is a polysilicon layer, suspended over 2.75 μm of air gap, followed below by a 0.6 μm thick silicon nitride layer and the doped silicon substrate, which is the bottom electrode. The plate dimensions are 340 μm x 340 μm and the pull-in voltage is 24.5 V. The parameters of the two-exponential charge dynamics model for this device, obtained from fittings of experimental data, are: $Q^n_{\max}/C_d = -4.67$ V, $Q^p_{\max}/C_d = 3.85$ V, $\tau^n_{C,1} = 0.33$ s, $\tau^p_{C,1} = 4.7$ s, $\tau^n_{C,2} = 2.11$ s, $\tau^p_{C,2} = 29.1$ s, $\tau^n_{D,1} = 0.98$ s, $\tau^p_{D,1} = 10.2$ s, $\tau^n_{D,2} = 89.1$ s, $\tau^p_{D,2} = 52.6$ s, $\zeta^n_1 = \zeta^p_1 = 0.61$, $\zeta^n_2 = \zeta^p_2 = 0.39$. The charge control method is implemented using a precision impedance analyzer, which performs the capacitance measurements and also applies the subsequent excitation waveform, BIT0 and BIT1, according to (3).

The control method was applied to achieve a set of values of ΔC_{th} ranging from -5fF to +5 fF in constant 1 fF steps. The values used in the BIT0 and BIT1 waveforms are $V^+ = -V^-$=10 V, T_s=180 ms and δ=1/7. The results obtained are summarized in Fig. 5. Each point of this figure corresponds to the following case: charge control is applied to set a given value of ΔC_{th}, thus a certain amount of net charge Q_d during 3 hours. This is time enough to reach stable control regimes in all cases considered, and allows one to obtain the asymptotic averaged bitstream that corresponds to such stable regime. Finally, all experiments were made for three different values of T_s, namely 180 ms, 820 ms and 1.7 s. Note that not all of these values are below the time constants reported above.

Accordingly to theoretical and simulation results discussed in previous sections, a plateau is clearly observed in Fig. 5 for the slowest rate T_s=1.7 s. This plateau "locks" to zero the bit stream average (same average number of BIT0's and BIT1's applied during the stable regime) for values of ΔC_{th} ranging from -2fF to +1fF. This means that, for this case, the control method is unable to distinguish ΔC_{th} and thus the corresponding target charge, within this range. Again, the size of the plateaus becomes reduced when the sampling frequency increases, as also seen in Fig. 5. In particular, note that the "charge locking" effect disappears, and thus there is a 'one to one' relationship between ΔC_{th} and the bitstream average, for the fastest sampling rate T_s=180 ms.

VI. Conclusions

The dynamics of a sigma-delta dielectric charge control has been discussed through simulations, analysis and experiments. The discrete time maps associated to the control method have been obtained assuming multiexponential dielectric charging models. The appearance of charge locking phenomena for low sampling frequencies has been analyzed. Experiments obtained with a parallel plate MEMS capacitor have confirmed the existence of plateaus and how they disappear as the sampling frequency is conveniently increased.

References

[1] W. M. V. Spengen, "Capacitive RF MEMS switch dielectric charging and reliability: a critical review with recommendations," *Journal of Micromechanics and Microengineering*, vol. 22, no. 7, p. 074001, 2012.

[2] W. de Groot, J. Webster, D. Felnhofer, and E. Gusev, "Review of device and reliability physics of dielectrics in electrostatically driven MEMS devices," *Device and Materials Reliability, IEEE Trans. on*, vol. 9, no. 2, pp. 190 –202, june 2009.

[3] Z. Peng, X. Yuan, J. Hwang, D. Forehand, and C. Goldsmith, "Dielectric charging of RF MEMS capacitive switches under bipolar control-voltage waveforms," in *IEEE/MTT-S Int. Microwave Symp.*, June 3-8 2007, pp. 1943 – 1946.

[4] T. Ikehashi, T. Miyazaki, H. Yamazaki, A. Suzuki, E. Ogawa, S. Miyano, T. Saito, T. Ohguro, T. Miyagi, Y. Sugizaki, N. Otsuka, H. Shibata, and Y. Toyoshima, "An RF MEMS variable capacitor with intelligent bipolar actuation," in *IEEE Int. Solid-State Circuits Conf. (ISSCC 2008)*, Feb 3-7, 2008, pp. 581–583.

[5] W. Wong and C. Lai, "Longer MEMS switch lifetime using novel dual-pulse actuation voltage," *IEEE Trans. on Device and Materials Reliability*, vol. 9, no. 4, 2009.

[6] M. Dominguez, D. Lopez, D. Molinero, and J. Pons, "Dielectric charging control for electrostatic MEMS switches," in *Proc. of SPIE Conf. on Defense, Security and Sensing DSS-20109, Orlando*, 2010.

[7] S. Gorreta, J. Pons-Nin, E. Blokhina, O. Feely, and M. Dominguez-Pumar, "Delta-sigma control of dielectric charge for contactless capacitive MEMS," *IEEE-JMEMS*, vol. 23, no. 4, pp. 829–841, Aug 2014.

[8] S. Gorreta, J. Pons-Nin, E. Blokhina, and M. Dominguez, "A second-order delta-sigma control of dielectric charge for contactless capacitive MEMS," *IEEE-JMEMS*, vol. 24, no. 2, pp. 259–261, 2015.

[9] G. Ding, D. Molinero, W. Wang, C. Palego, S. Halder, J. Hwang, and C. L. Goldsmith, "Intelligent bipolar control of mems capacitive switches," *Microwave Theory and Techniques, IEEE Trans. on*, vol. 61, no. 1, pp. 464–471, 2013.

[10] P. Giounanlis, E. Blokhina, O. Feely, S. Gorreta, J. Pons-Nin, and M. Domnguez, "Sigma-Delta inspired control technique for the improvement of MEMS reliability," in *International Symposium on Circuits and Systems, Melbourne*, June 1-5 2014.

[11] X. Rottenberg, I. De Wolf, B. Nauwelaers, W. De Raedt, and H. A. C. Tilmans, "Analytical model of the dc actuation of electrostatic MEMS devices with distributed dielectric charging and nonplanar electrodes," *IEEE-JMEMS*, vol. 16, no. 5, pp. 1243–1253, 2007.

[12] G. Papaioannou and J. Papapolymerou, "Dielectric charging mechanisms in RF-MEMS capacitive switches," in *Microwave Integrated Circuit Conference, 2007. EuMIC 2007. European*, Oct 2007, pp. 359–362.

[13] E. Blokhina, S. Gorreta, D. Lopez, D. Molinero, O. Feely, J. Pons-Nin, and M. Dominguez-Pumar, "Dielectric charge control in electrostatic MEMS positioners/varactors," *IEEE-JMEMS*, vol. 21, no. 3, pp. 559 –573, June 2012.

[14] H. Bruin and J. Deane, "Piecewise contractions are asymptotically periodic," *Proceedings of the American Mathematical Society*, vol. 137, no. 4, pp. 1389 – 1395, 2009.

[15] O. Feely and L. Chua, "The effect of integrator leak in $\Sigma\Delta$ modulation," *IEEE Trans. on Circuits and Systems I*, vol. 38, pp. 1293–1305, 1991.

[16] M. Dominguez-Pumar, S. Gorreta, and J. Pons-Nin, "Slide mode analysis of the dynamics of sigma-delta controls of dielectric charging," *IEEE Trans. on Industrial Electronics*, 2016.